THE PROTEIN SOCIETY

Kinetics and thermodynamics of metal-binding to histone deacetylase 8

Byungchul Kim,[1] Amit S. Pithadia,[2] and Carol A. Fierke[1,2,3]*

[1]Chemical Biology Program, University of Michigan, Ann Arbor, Michigan 48109-2216
[2]Department of Chemistry, University of Michigan, Ann Arbor, Michigan 48109-1055
[3]Department of Biological Chemistry, University of Michigan Medical School, Ann Arbor, Michigan 48109-0600

Received 5 November 2014; Accepted 8 December 2014
DOI: 10.1002/pro.2623
Published online 16 December 2014 proteinscience.org

Abstract: Histone deacetylase 8 (HDAC8) was originally classified as a Zn(II)-dependent deacetylase on the basis of Zn(II)-dependent HDAC8 activity *in vitro* and illumination of a Zn(II) bound to the active site. However, *in vitro* measurements demonstrated that HDAC8 has higher activity with a bound Fe(II) than Zn(II), although Fe(II)-HDAC8 rapidly loses activity under aerobic conditions. These data suggest that in the cell HDAC8 could be activated by either Zn(II) or Fe(II). Here we detail the kinetics, thermodynamics, and selectivity of Zn(II) and Fe(II) binding to HDAC8. To this end, we have developed a fluorescence anisotropy assay using fluorescein-labeled suberoylanilide hydroxamic acid (fl-SAHA). fl-SAHA binds specifically to metal-bound HDAC8 with affinities comparable to SAHA. To measure the metal affinity of HDAC, metal binding was coupled to fl-SAHA and assayed from the observed change in anisotropy. The metal K_D values for HDAC8 are significantly different, ranging from picomolar to micromolar for Zn(II) and Fe(II), respectively. Unexpectedly, the Fe(II) and Zn(II) dissociation rate constants from HDAC8 are comparable, k_{off} ~0.0006 s^{-1}, suggesting that the apparent association rate constant for Fe(II) is slow (~3 × 10^3 M^{-1} s^{-1}). Furthermore, monovalent cations (K^+ or Na^+) that bind to HDAC8 decrease the dissociation rate constant of Zn(II) by ≥100-fold for K^+ and ≥10-fold for Na^+, suggesting a possible mechanism for regulating metal exchange *in vivo*. The HDAC8 metal affinities are comparable to the readily exchangeable Zn(II) and Fe(II) concentrations in cells, consistent with either or both metal cofactors activating HDAC8.

Keywords: histone deacetylase 8; fl-SAHA; metal-binding mechanism; monovalent cations

Introduction

Misregulation of posttranslational modifications are implicated in many human diseases, including cancer and neurodegenerative diseases.[1] Post-translational acetylation of lysine side chains has been observed at more than 3600 sites in proteins, including histones,[2,3] and this modification regulates the biological activity of many of these proteins. For example, acetylation and deacetylation correlate with the activation and deactivation, respectively, of transcriptional gene expression. The acetylation status of lysine residues is reversibly regulated by histone acetyltransferase (HAT) and histone deacetylase (HDAC) activities. HDACs are a family of 18 enzymes grouped into four classes. Class I, II, and IV are metalloenzymes with a largely conserved catalytic core, consistent with a common catalytic

Abbreviations: c-SAHA, coumarin-suberoylanilide hydroxamic acid; CAII, carbonic anhydrase II; DVC, divalent cation; EDTA, ethylenediaminetetraacetic acid; FdL, fluor de Lys; fl-SAHA, fluorescein-labeled suberoylanilide hydroxamic acid; FP, fluorescence polarization; HAT, histone acetyltransferase; HDAC, histone deacetylase; HEPES, 4-(2-hydroxyethyl)-1-piperazineethanesulfonic acid; ICP-MS, inductively coupled plasma mass spectrometry; LpxC, UDP-3-*O*-[(*R*)-3-hydroxymyristoyl]-*N*-acetylglucosamine deacetylase; LuxS, *S*-ribosylhomocysteine lyase; MOPS, 3-(*N*-morpholino)-propanesulfonic acid; MVC, monovalent cation; NTA, nitrilotriacetic acid; PDF, peptide deformylase.

Grant sponsor: National Institutes of Health (NIH); Grant number: GM40602 (to C.A.F.).

*Correspondence to: Carol Fierke, Department of Chemistry, University of Michigan, 930 N University, Ann Arbor, MI 48109. E-mail: fierke@umich.edu

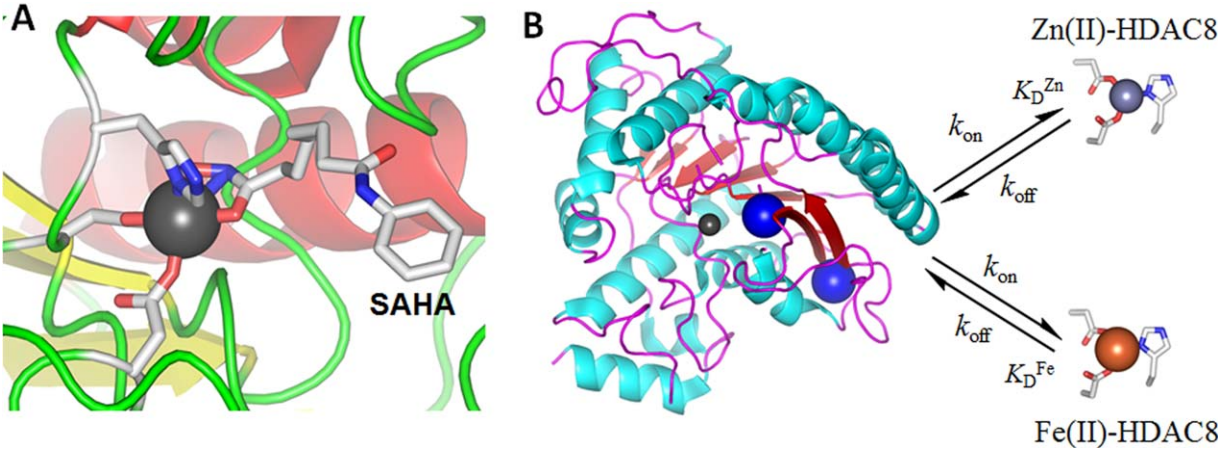

Figure 1. Structure of HDAC8. Catalytic activity of HDAC8 is activated by either Zn(II) or Fe(II)11. (A) A close-up of HDAC8 active site showing the HisAsp2 metal coordination sphere with bound SAHA (PDB ID: 1T69). (B) Crystal structure of HDAC8 displaying divalent cation (black sphere) and two monovalent cation (blue spheres) binding sites (PDB ID: 2V5W).[12] The active site metal could either be Zn(II) (PDB: 3EW8) or Fe(II) (PDB ID: 3MZ6)[10] and selectivity is governed by kinetic and thermodynamic values.

mechanism.[4] Class I comprises four HDAC family members, HDAC 1, 2, 3, and 8, which are expressed ubiquitously and generally display deacetylase activity toward histone substrates.[5] Class II includes HDAC 4, 7, 9, and 10 which generally have lower catalytic activity. HDAC11, the sole member of class IV, lies at the boundary between the other two HDAC classes. All three classes are distinct from the sirtuin-family of enzymes (class III) in the catalytic domain sequence, three-dimensional structure, and catalytic mechanism.[6]

High-resolution crystal structures of the histone deacetylase-like protein from *Aquifex aeolicus*, human HDAC8, and *Schistosoma mansoni* HDAC8 have been solved illustrating a single α/β domain with a core eight-stranded β-sheet surrounded by 11 α-helices.[7–11] The substrate binding surface is composed of nine loops and an 11 Å tunnel leading to the active site that includes a $HisAsp_2$ divalent metal binding site [Fig. 1(a)]. These crystal structures were solved primarily with zinc(II) as the active site metal ion, although little change in the inhibitor-bound structure of HDAC8 was observed with other metals (Co(II), Fe(II), and Mn(II)) bound in the active site.[9] Nonetheless, the enzymatic activity of HDAC8 varies with the active site metal ion, Co(II) > Fe(II) > Zn(II) > Ni(II), using the commercial HDAC8 substrate.[13]

Previous research has demonstrated that HDAC8 is activated by either Fe(II) or Zn(II) *in vitro* and, possibly, *in vivo*. The k_{cat}/K_M value for deacetylation of a Fluor de Lys peptide catalyzed by HDAC8 stoichiometrically substituted with metals is 3-fold greater for Fe(II) compared with Zn(II). Furthermore, for recombinant expression of HDAC8 in *E. coli*, the HDAC8 activity in cell-free lysates is approximately fourfold higher under anaerobic conditions than under aerobic conditions and both Zn and Fe co-purify with the protein.[13] Finally, the active site metal ligands of HDAC8 ($HisAsp_2$) are unusual for a zinc-dependent hydrolase.[9,14–16] These findings suggest that HDACs could potentially be activated by Fe(II) rather than Zn(II) *in vivo* [Fig. 1(b)]. There have been several examples of Zn(II)-dependent hydrolases that have been reclassified as "Fe(II)-dependent" enzymes, including peptide deformylase (PDF), *S*-ribosylhomocysteine lyase (LuxS), and UDP-3-*O*-[(*R*)−3-hydroxymyristoyl]-*N*-acetylglucosamine deacetylase (LpxC).[17–19] In particular, pulldown and metal analysis experiments of the metal-dependent deacetylase LpxC demonstrated that this protein binds mainly Fe(II) in *Escherichia coli* cells, despite the weaker affinity for Fe(II) compared with Zn(II) (K_D for Fe(II) and Zn(II) is 0.1 μ*M* and 60 p*M*, respectively).[19,20] The data thus far suggest that HDAC8 may fall into this category as well. A detailed understanding of the metal binding kinetics and thermodynamics will provide insight into the native cofactor.

To date, a number of HDAC activity assays have been developed to measure peptide reactivity (k_{cat}/K_M) and inhibitor potency (K_i).[21,22] Recently, a fluorescence-based binding assay has been developed using coumarin-suberoylanilide hydroxamic acid (c-SAHA) as the fluorescent probe. However, the fluorescence of this ligand is only quenched 50% upon binding to HDAC8[23] and the coumarin fluorophore ($\lambda_{ex} = 325$ nm, $\lambda_{ex} = 400$ nm) is unsuitable for fluorescence polarization (FP) measurements due to a short lifetime.[24] To develop an anisotropy (or polarization)-based assay, we synthesized fluorescein-labeled SAHA (fl-SAHA) as a small molecule probe. Fluorescein as the fluorophore has high quantum yield, good photostability, a large Stokes shift, and a

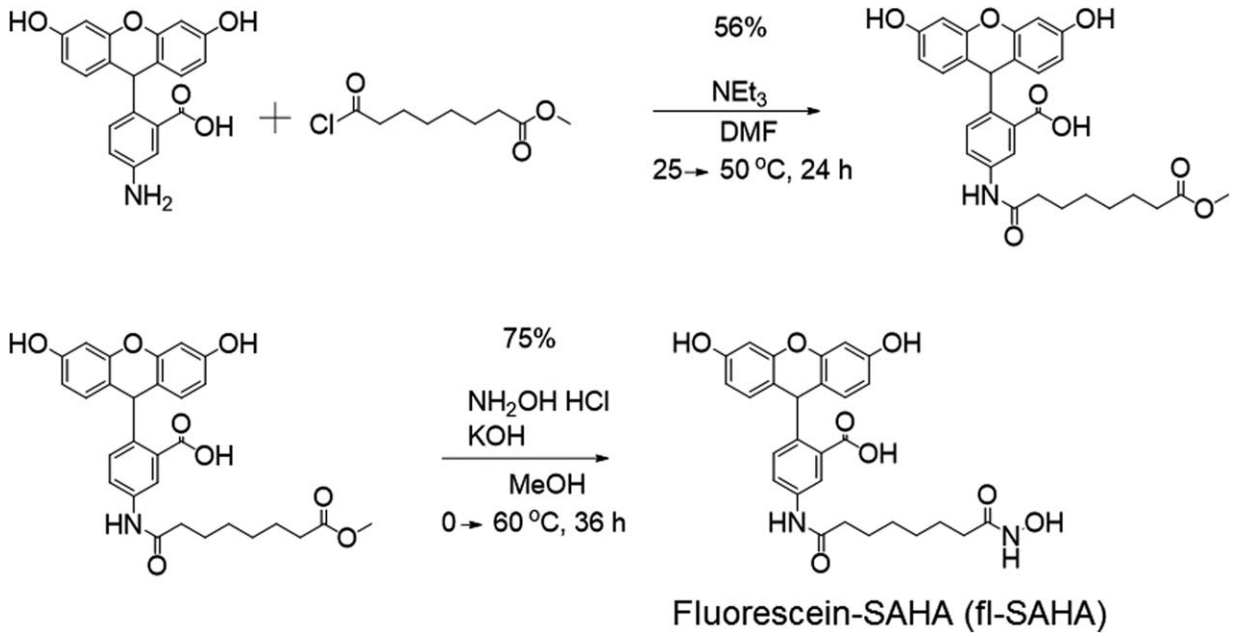

Figure 2. Synthetic scheme of fluorescein-SAHA (fl-SAHA).

lifetime in the correct range for measuring binding to proteins using changes in anisotropy or polarization.[25–27] Furthermore, coupling of the binding of fl-SAHA to metal binding to HDAC8 allows measurement of metal affinity from changes in fluorescence polarization in a 96-well format with ease and precision since it is a ratiometric measurement. Furthermore, in a competition format this assay is also applicable for high-throughput screening for inhibitors against HDAC8.

Herein the affinity of HDAC8 for Zn(II) is determined to be much higher (5 p*M*) than the Fe(II) affinity (0.2 μ*M*), as predicted based on the Lewis acidity of Zn(II) compared with Fe(II) and in accordance with the Irving-Williams series of stability constants.[28] Although, the total cellular concentrations of zinc and iron are comparable at 0.1 to 0.2 m*M* in eukaryotes and *E. coli*,[29,30] the readily exchangeable (RE) metal ion concentrations differ significantly; $[Zn(II)]_{RE}$ has been measured in the picomolar range (10–400 p*M*)[31–33] in both eukaryotes and prokaryotes,[30] while the best estimate for $[Fe(II)]_{RE}$ is micromolar (0.2–6 μ*M*) in eukaryotic cells.[34–37] Therefore, based on thermodynamic considerations, it is possible that HDACs could be activated by Fe(II) rather than Zn(II) in eukaryotic cells.

We also demonstrate that monovalent cations bound to HDAC8 play a role in regulating metal equilibrium kinetics. Finally, the metal dissociation rate constant is comparable for zinc and iron, suggesting a two-step metal association mechanism. These studies measuring the metal kinetics and thermodynamics of HDAC8 provide insight into the feasibility and biological relevance of the regulation of HDAC8 activity by mono- and divalent cations.

Results

Design of a Fluorescein-SAHA Probe for HDAC8

Recently, the pan-HDAC inhibitor, SAHA, was derivatized with a coumarin fluorophore to form coumarin-suberoylanilide hydroxamic acid (c-SAHA).[23] The fluorescence of this molecule is quenched 50% upon binding to HDAC8 and this property has been used to measure the binding kinetics for HDAC inhibitors.[38] However, the modest change in the fluorescence intensity limits the utility of this approach for measuring the affinity of HDAC ligands. Therefore, we developed a fluorescence polarization probe by coupling a fluorescein derivative (6-aminofluorescein) to SAHA to form fl-SAHA (Fig. 2). We have analyzed the affinity of this inhibitor for HDAC8 and used this probe to measure the metal binding affinity of HDAC8 for Zn(II) and Fe(II).

Binding affinity of apo and metal-bound HDAC8 for fluorescein-SAHA

To probe the affinity of fl-SAHA for metal-bound HDAC8, we measured the fluorescence anisotropy of fl-SAHA upon titration with bovine serum albumin (BSA), apo or metal-bound HDAC8 under equilibrium conditions in assay buffer (20 m*M* HEPES, pH 8, 137 m*M* NaCl, and 3 m*M* KCl, Fig. 3). Upon addition of metal-bound HDAC8, the fluorescence anisotropy increased with a hyperbolic dependence on the HDAC8 concentration, as predicted for binding of a small molecule to the larger protein ($M_W = 42.5$ kDa). A quadratic fit to these data allows calculation of a dissociation constant of fl-SAHA (K_D) from Zn-bound and Fe-bound HDAC8 of 0.4 ± 0.1 μ*M* and

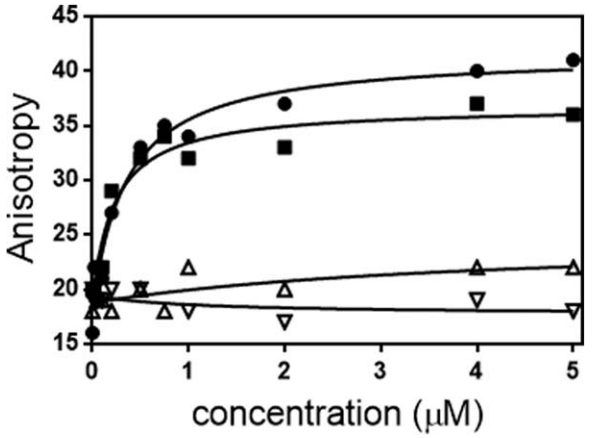

Figure 3. Metal dependence of HDAC8 affinity for fl-SAHA. Measurement of the binding affinity (K_D) of apo-(Δ), Zn(II)-bound (•), or Fe(II)-bound (■) HDAC8 for fl-SAHA from changes in fluorescence anisotropy (λ_{ex} =485 nm, λ_{em} = 535 nm) upon addition of protein to 50 n*M* fl-SAHA in 20 m*M* HEPES, pH 8, 137 m*M* NaCl, and 3 m*M* KCl, at 25°C. As a control, BSA (▽) was titrated into fl-SAHA. The anisotropy values are adjusted for a modest decrease in the total fluorescence. The K_D of Zn-HDAC8 and Fe-HDAC8 for fl-SAHA are calculated as 0.4 ± 0.1 μ*M* and 0.1 ± 0.08 μ*M*, respectively, from a fit of Eq. (1) to the data (solid lines). Little change in anisotropy is observed for addition of either apo-HDAC8 or BSA.

0.10 ± 0.08 μ*M*, respectively (Table I). Little or no change in fluorescence anisotropy was observed upon titration of fl-SAHA with BSA or apo-HDAC8; the affinity for apo-HDAC8 for fl-SAHA can be estimated ($K_D > 20$ μ*M*) assuming a constant anisotropy endpoint. This result indicates that the affinity of HDAC8 for fl-SAHA is enhanced >10-fold by interaction with the bound divalent metal ion. Therefore, fl-SAHA can be used as a probe to visualize metal-bound HDAC8 and to interrogate metal selectivity and affinity.

Rate constant for dissociation of fl-SAHA complexed with HDAC8

To measure the dissociation rate constant for fl-SAHA, the HDAC8•fl-SAHA complex was mixed with excess unlabeled SAHA to rapidly bind to and trap HDAC8 upon dissociation of fl-SAHA. The replacement of SAHA for fl-SAHA bound to HDAC8 leads to both a decrease in the fluorescence anisotropy and an increase in the fluorescent intensity (λ_{ex} = 495 nm, $\lambda_{em} > 500$ nm), allowing measurement of the fl-SAHA dissociation rate constant. The time-dependent increase in fluorescence observed after mixing the metal-bound HDAC8•fl-SAHA complex with 20 μ*M* SAHA in the stopped-flow fluorometer (Fig. 4) is well-described by a single exponential with fl-SAHA dissociation rate constants of 0.62 ± 0.06 and 0.036 ± 0.001 s^{-1} for Zn(II)-bound and Fe(II)-bound HDAC8, respectively (Table I). These rate constants are unchanged when the concentration of SAHA is increased by twofold (data not shown), demonstrating that trapping of HDAC8 by SAHA is rapid and therefore the measured rate constant reflects dissociation of fl-SAHA.

Metal binding properties of HDAC8

Zn(II) and Fe(II) are the most likely native cofactors that activate HDAC8 *in vivo* since they exist in high concentrations in the cell.[29] The binding affinities (K_D) of HDAC8 for Zn(II) and Fe(II) were measured from the metal-dependent activation of catalytic activity using the FdL assay as a function of free metal concentration [Fig. 5(a) and Table II, $K_{D,Zn}$ = 5 ± 1 p*M* and $K_{D,Fe}$ = 0.19 ± 0.03 μ*M*]. These values are slightly lower than previously measured metal affinities for HDAC8.[9] This method requires that the metal complex has significant catalytic activity. In contrast, metal affinity could be measured for inactive complexes by coupling metal binding to fl-SAHA binding. To validate this method, the fluorescence anisotropy of fl-SAHA in the presence of HDAC8 was measured as a function of free metal concentration in nitrilotriacetate (NTA)-buffered solutions under equilibrium conditions. The fluorescence anisotropy increases with a hyperbolic dependence on the free metal concentration [Fig. 5(b)] while the total fluorescence intensity decreases less than twofold (data not shown). Dissociation constants (K_D) were obtained from fitting a single binding isotherm to these data ($K_{D,Zn}$ = 6 ± 1 p*M* and $K_{D,Fe}$ = 0.2 ± 0.1 μ*M*), in agreement with the affinity measurements using the FdL assay. These data confirm that HDAC8 has significantly higher affinity for Zn(II) compared with Fe(II), consistent with the higher Lewis acidity of Zn(II).[39]

To examine the metal binding kinetics, the rate constants for dissociation (k_{off}) of the HDAC8-bound metal ion were determined from the time-dependent decrease in activity upon dilution of the enzyme into

Table I. *Kinetic Parameters of fl-SAHA Binding to Zn(II)- or Fe(II)-HDAC8*

	$K_D^{fl\text{-}SAHA}$ (μ*M*)[a] measured	k_{off} (s^{-1})[b] measured	k_{on} (M^{-1} s^{-1})[c] calculated
Zn(II)-HDAC8	0.4 ± 0.1	0.62 ± 0.06	4 × 10^5
Fe(II)-HDAC8	0.10 ± 0.08	0.036 ± 0.001	1 ×10^5

[a] Measured using the FP assay in 20 m*M* HEPES, pH 8, 137 m*M* NaCl, and 3 m*M* KCl, at 25°C.
[b] Measured using stopped-flow fluorometry using the same conditions as in a.
[c] k_{on} calculated from k_{off}/K_D.

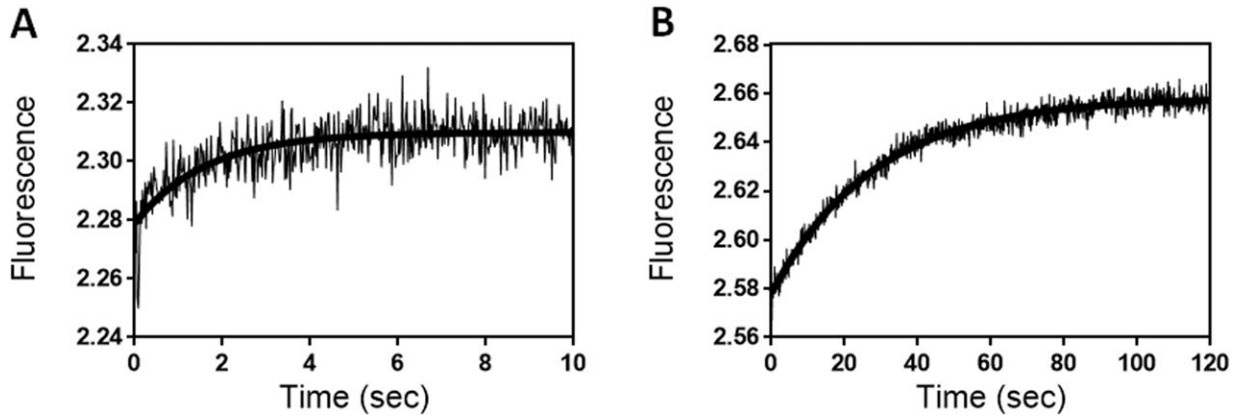

Figure 4. Rate constant for dissociation of fl-SAHA complexed with HDAC8. The dissociation rate constant (k_{off}) for fl-SAHA bound to metal-bound HDAC8 was measured using a stopped-flow fluorometer from a time-dependent increase in fluorescence intensity ($\lambda_{ex} = 495$ nm) after mixing the HDAC8•fl-SAHA complex with an equal volume of SAHA (final concentrations: 1 μ*M* M^{2+}-HDAC8, 0.05 μ*M* fl-SAHA, 20 μ*M* SAHA) in 20 m*M* HEPES, pH 8, 137 m*M* NaCl, and 3 m*M* KCl. For Fe(II)-bound HDAC8, apo HDAC8 was reconstituted with stoichiometric Fe(II) in the presence of 5 m*M* ascorbic acid. The solid lines are the best fit of a single exponential rate equation to the data: (A) Zn-HDAC8; $k_{off} = 0.6 \pm 0.06$ s^{-1} and (B) Fe-HDAC8: $k_{off} = 0.04 \pm 0.0005$ s^{-1}.

the high affinity metal chelator, EDTA, using the FdL assay (Fig. 6). The measured rate constants are not dependent on the concentration of EDTA (data not shown), indicating that the metal chelator is trapping the metals after dissociation from the enzyme. These measurements revealed that the rate constants for dissociation (k_{off}) of Zn(II) and Fe(II) from HDAC8 are 0.038 ± 0.003 and 0.034 ± 0.004 min^{-1}, respectively (Table II). The similarity in the dissociation rate constants for Zn(II) and Fe(II) is unexpected given the significantly different affinities of HDAC8 for these metal ions.

The discrimination between the affinities of the two metal ions by HDAC8 originates mainly from alterations in the apparent association rate constants (k_{on}^{app}). Assuming a one-step metal binding mechanism, the values for k_{on}^{app} can be estimated from the K_D and k_{off} values ($k_{on}^{app} = k_{off}/K_D$) as 1×10^8 M^{-1} s^{-1} (Zn(II)) and 3×10^3 M^{-1} s^{-1} (Fe(II)) (Table II). The estimated association rate constant for zinc binding to HDAC8 is near the diffusion-controlled limit, consistent with a single-step binding mechanism. However, the association rate constant for Fe(II) is orders of magnitude slower than the diffusion-limit ($\sim 10^8$ M^{-1} s^{-1})[40] suggesting a minimal kinetic mechanism for HDAC8 binding Fe(II) that includes two sequential steps, possibly a bimolecular diffusion-controlled association reaction

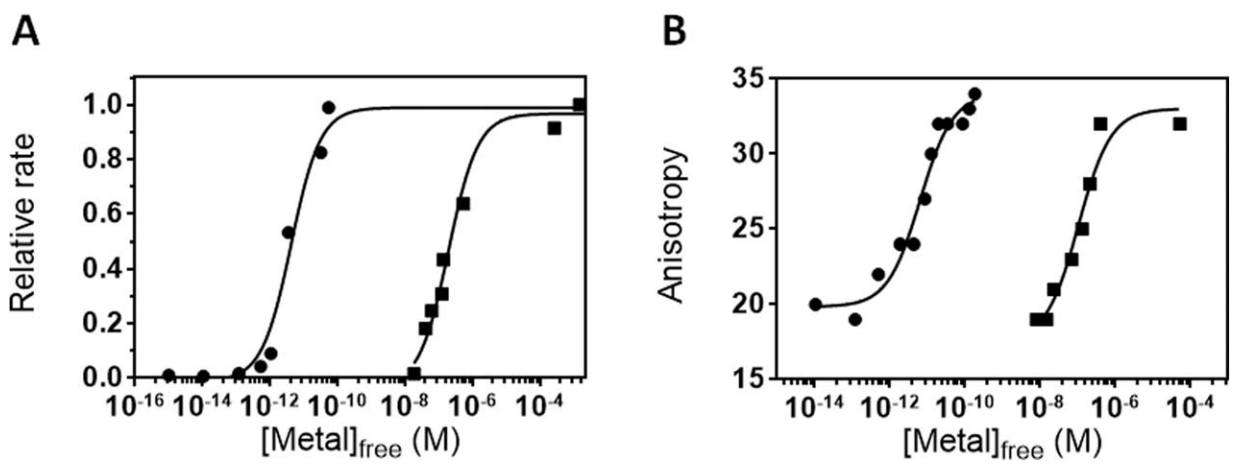

Figure 5. Measurement of metal affinity (K_D) of HDAC8 using the FdL activity and the anisotropy assays. HDAC8 (1 μ*M*) was incubated with increasing concentration of free Zn(II) (●) or Fe(II) (■) using a 1 m*M* NTA metal buffer in the presence of 3 m*M* KCl and 137 m*M* NaCl. The measurements with Fe(II) were carried out in an anaerobic chamber. (A) The activity was measured using the FdL assay and the relative initial velocity (v_{obs}/v_{max}) is plotted. (B) The anisotropy is measured in the presence of 50 n*M* fl-SAHA at varying free metal concentrations. The metal dissociation constants were determined from fitting a single binding isotherm [Eq. (3)] to these data.

Table II. *Kinetic Parameters for Metal Binding to HDAC8*

	$K_D^{metal,\ a}$ measured	k_{off} (min^{-1})[b] measured	k_{on}^{app} ($M^{-1}\ s^{-1}$)[c] calculated
Zn(II)-HDAC8	5 ± 1 p*M*	0.038 ± 0.003	1×10^8
Fe(II)-HDAC8	0.19 ± 0.03 μ*M*	0.034 ± 0.004	3×10^3

[a] Measured using the FdL and the FP assays in 20 m*M* HEPES, pH 8, 137 m*M* NaCl, and 3 m*M* KCl at 25°C.
[b] Measured using the FdL assay in 1 m*M* EDTA, 20 m*M* HEPES, pH 8, 3 m*M* KCl, and 137 m*M* NaCl at 25°C.
[c] k_{on} calculated from k_{off}/K_D.

to form an initial encounter complex followed by a unimolecular rearrangement to form the final HDAC8•metal complex (Scheme 1).

Monovalent cations modulate zinc dissociation kinetics

Crystal structures show that HDAC8 has binding sites for two MVCs, in addition to the divalent catalytic metal ion, which have been designated as site 1 (7 Å from the divalent catalytic metal ion) and site 2 (21 Å from the divalent catalytic metal ion) [Fig. 1(b)].[41,42] The MVC could be either K^+ or Na^+ based on their intracellular concentrations.[43,44] Previous research demonstrated that one bound MVC activates catalytic activity ($K_{1/2} = 14$ m*M* for K^+), whereas the second, weaker-binding MVC ($K_{1/2} = 130$ m*M* for K^+) decreases catalytic activity.[45] Mutagenesis data suggest that the MVC bound to site 1 inhibits catalytic activity, likely by altering the pK_a of His-142, whereas the site 2 MVC enhances activity, likely by an allosteric effect.[45] These data suggest that HDAC8 may be regulated by cations *in vivo*. In smooth muscle cells where the cytosol contains 100 m*M* KCl and 4 m*M* NaCl,[46,47] potassium ions are predicted to partially inhibit the activity of HDAC8.

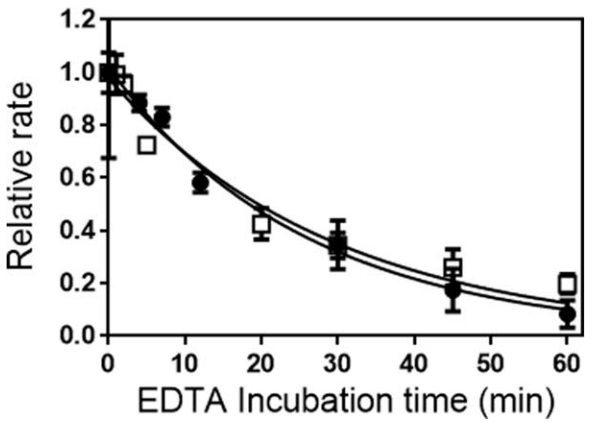

Figure 6. Measurement of the metal dissociation rate constant (k_{off}) from the HDAC8•Me(II) complex using the FdL activity assay. The k_{off} values for HDAC8-bound metal ions were determined from the time-dependent decrease in activity measured using the FdL assay after dilution of either Zn(II)-(●) or Fe(II)-(□) HDAC8 (final concentration = 1 μ*M*) into 1 m*M* EDTA in 20 m*M* HEPES, pH 8, 3 m*M* KCl, 137 m*M* NaCl, 25°C. The solid lines are a single exponential fit to the data.

To evaluate whether MVCs bound to HDAC8 also regulate the metal equilibration kinetics, the HDAC8 zinc dissociation rate constant (k_{off}) was measured as a function of the concentration of either K^+ or Na^+. As the MVC concentration increases, the observed value of k_{off} decreases by >100-fold for K^+ and >10-fold for Na^+ (Fig. 7). These data were analyzed using a model where the MVC binds to HDAC8 and decreases the metal dissociation rate constant [Scheme 2; Eq. (4)] leading to an apparent dissociation constant of 1 m*M* and 93 m*M*, for K^+ and Na^+, respectively, with little or no observable cooperativity ($n = 1$ and 1.2 for K^+ and Na^+). These data indicate that this MVC site will be saturated under most *in vivo* sodium and potassium concentrations. These results also suggest that binding a single MVC to HDAC8 is sufficient to decrease the metal dissociation rate constant; there is no evidence that binding to the second MVC site alters metal dissociation. This is in contrast to the differential effects of the MVCs on catalytic activity. Additionally, the apparent K^+ dissociation constant calculated from the decrease in the zinc dissociation rate constant is significantly (~14-fold) lower than the value determined from activation of catalytic activity. This could reflect difficulties in measuring activity at low potassium concentrations.[45] The decrease in the zinc dissociation rate data suggest that MVCs may increase the affinity of HDAC8 for Zn(II), assuming little effect on the association rate constant.

Discussion

HDAC8 is activated by a number of divalent metal ions, including Zn(II), Fe(II), Ni(II), and Co(II) *in vitro*,[13] however, the metal ion that activates this class of enzymes in cells is not yet known. The use of Fe(II) as the physiological catalytic metal ion has been previously demonstrated for multiple metallohydrolases, such as peptide deformylase, methionyl aminopeptidase, LuxS, γ-carbonic anhydrase, cytosine deaminase, and atrazine chlorohydrolase.[17,18,48–51]

$$E + M^{2+} \underset{k_2}{\overset{k_1}{\rightleftharpoons}} EM^{2+} \underset{k_4}{\overset{k_3}{\rightleftharpoons}} E^*M^{2+}$$

Scheme 1. Minimal kinetic mechanism of metal binding to HDAC8.

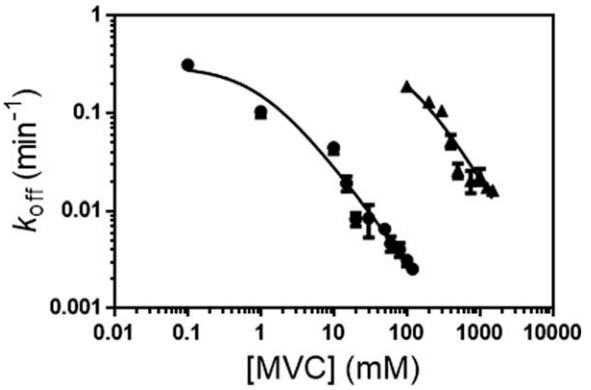

Figure 7. Dependence of metal dissociation rate constant (k_{off}) from the HDAC8•Zn(II) complex on the concentration of monovalent cations. The rate constants were determined as described in the legend of Figure 6. The values for k_{off} decrease at increasing concentrations of KCl (●) or NaCl (▲). The solid line is a fit of Eq. (4) to the data.

These enzymes were originally misidentified as Zn(II)-metalloenzymes due to purification under aerobic conditions resulting in replacement of the oxygen-sensitive Fe(II) with the higher affinity Zn(II) cofactor. The oxygen sensitivity of HDAC8 activity in *E. coli* cell lysates originally suggested that HDAC8 may be another non-heme Fe(II) hydrolase that was previously identified as a zinc metalloenzyme.[13] Similarly, the deacetylase activity of endogenously expressed HDAC8 isolated from HeLa cells by immunoprecipitation decreased upon exposure to oxygen (approximately twofold), suggesting that HDAC8 is partially Fe-bound.[52] These data are consistent with activation of HDAC8 by a Fe(II) metal cofactor under many physiological conditions.

An interesting possibility is that the metal ion bound to HDAC8 may depend on the readily exchangeable concentrations of Fe(II) and Zn(II); the bound Fe(II) metal ion may exchange with zinc under conditions where the cellular zinc concentration increases significantly, such as oxidative stress,[32] or due to the activity of metallochaperones.[32,53–55] While metallochaperones for Zn have not yet been identified, the Philpott lab has demonstrated that poly r(C)-binding protein 1 (PCBP1) functions as a cytosolic iron chaperone in *Saccharomyces cerevisiae* to deliver iron to ferritin, a cellular iron storage protein, as well as several hydroxylases.[56–58] A recent mass spectrometric analysis

$$\text{E-Zn-MVC} \overset{K_{eq}}{\rightleftharpoons} \text{E-Zn} + \text{MVC}$$
$$\downarrow k_{off}$$
$$\text{E} + \text{Zn} + \text{MVC}$$

Scheme 2. Coupled binding of MVC and DVC to HDAC8.

evaluating HDAC8 protein binding partners suggested interactions with the PCBP family of iron-metallochaperones.[59]

To further explore metal activation of HDAC8 we have measured the metal binding kinetics and thermodynamics of HDAC8 using the FdL activity assay and an FP assay using a new fluorescent probe (fl-SAHA). Notably, this FP assay can be used to measure the metal binding kinetics and thermodynamics of HDAC8 in the absence of catalytic activity, allowing analysis of metal affinity in a wide variety of conditions and with mutant enzymes. This assay could also be developed as a high-throughput screen for HDAC inhibitors and, potentially, for imaging HDAC8 in cells since anisotropy measurements are ratiometric.[60–63]

fl-SAHA binds to metal-bound HDAC8 in the submicromolar range (0.4 μM for Zn(II)-bound and 0.1 μM for Fe(II)-bound), which is comparable to both SAHA ($K_I = 0.3$ μM for Zn(II) and 0.1 μM for Fe(II)-bound HDAC8[13]) and coumarin-conjugated SAHA (0.2 μM for HDAC8).[23] This is reasonable since both SAHA analogs contain the same aliphatic hydroxamate moiety that chelates the active site metal ion and can be accommodated in the hydrophobic tunnel of HDAC8.[41] Additionally, fl-SAHA displays similar K_D values for the Zn(II)- and Fe(II)-bound HDAC8 forms, as previously observed for SAHA.[13] Dissociation rate constants (k_{off}) of fl-SAHA from metal-bound HDAC8 were determined using stopped-flow spectrometry as 0.6 s^{-1} and 0.04 s^{-1} for Zn(II)- and Fe(II)-HDAC8, respectively. Apparent association rate constants of fl-SAHA to metal-bound HDAC8 were calculated as 4×10^5 M^{-1} s^{-1} and 1×10^5 M^{-1} s^{-1} for Zn(II)- and Fe(II)-HDAC8, respectively, assuming it is a single-binding step mechanism (Table I). The differential effects of metal-substitution on the association rate constants may suggest a multistep binding mechanism.

The affinity of HDAC8 for Zn(II) is 10^5-fold higher than Fe(II), as measured by either the fl-SAHA FP assay or metal-dependent activation of catalytic activity ($K_{D,Zn} = 5 \pm 1$ pM and $K_{D,Fe} = 0.19 \pm 0.03$ μM).[9] However, the picomolar and micromolar affinities of HDAC8 for Zn(II) and Fe(II), respectively, are in the range of estimated concentrations of readily exchangeable metal ions in cells.[9,31,32,37] This similarity suggests that HDAC8 might be poised to switch between Fe(II)- and Zn(II)-bound states in cells. Unexpectedly, the dissociation rate constants (k_{off}) of both metals (0.0006 s^{-1}) are similar, despite the difference in the binding affinities. This result indicates that metal selectivity primarily resides in the apparent association rate constant, estimated as 10^8 and 10^3 M^{-1} s^{-1} for Zn(II) and Fe(II), respectively, assuming a single association step (Table II). The low value for the apparent association rate constant for Fe(II)

suggests that metal association is a two-step mechanism (Scheme 1) where an initial encounter complex forms followed by a unimolecular rearrangement to form the final Me(II)-metal complex. This two-step mechanism may describe both Zn(II) and Fe(II) binding to HDAC8 with different rate-limiting steps; formation of the encounter complex may be the slow step for Zn(II) binding (k_1) while the rearrangement step may be rate-limiting for Fe(II) binding (k_1k_3/k_2). Metal dissociation could be limited in both cases by the reverse rearrangement step (k_4).

Previously, the metal association kinetics of human carbonic anhydrase II (CAII) were determined with estimated association rate constants for Zn(II) and Cu(II) of 10^4 to 10^5 and 10^9 M^{-1} s^{-1}, respectively.[64] These data along with analysis of the zinc binding kinetics of CAII mutants suggest a two-step binding mechanism.[64,65] In the first step, zinc binds to CAII at near diffusion-controlled rates to form an initial complex with two protein ligands followed by a second slower step that includes exchange of inner-sphere water molecules with the third protein ligand.[64] This may be a paradigm for two-step metal binding to proteins, including HDAC8. Metal binding kinetics similar to HDAC8 have been measured for the bacterial deacetylase, LpxC, where the apparent association rate constants for Zn(II) and Fe(II) are estimated as 10^6 and 10^4 M^{-1} s^{-1}, respectively, also suggesting a two-step binding mechanism for metal association.[19] In this case, the physiologically relevant metal of LpxC in *E. coli* is Fe(II) under most conditions, although LpxC binds Zn(II) *in vivo* when Fe(II) concentrations are very low. In LpxC and CAII, the physiological metal ions (Fe(II) and Zn(II), respectively) have a slow dissociation rate constant (LpxC for Fe(II) $k_{off} = 0.067 \pm 0.004$ min^{-1} and CAII for Zn(II) $k_{off} = 8.5 \pm 0.3 \times 10^{-5}$ min^{-1}), leading to an apparent association rate constant that is slower than the diffusion-controlled limit.[19,65] The varied dissociation rate constants may be important for metal selectivity *in vivo*, decreasing kinetic traps for the higher affinity, but incorrect metal ion, such as Zn(II) for LpxC and possibly HDAC8 or Cu(II) for CAII.[19,66] Furthermore, the similarities between the *in vitro* metal binding kinetics and thermodynamics of LpxC and HDAC8 fuel the hypothesis that HDAC8 might be activated by Fe(II) under most conditions but switches to the Zn(II) bound enzyme at high levels of cellular zinc.[19] This model suggests the possibility of regulation of the activity of HDAC8 by metal switching in response to conditions that alter the cellular concentration of readily exchangeable metal concentrations, such as redox stress.

The crystal structure of HDAC8 also displays two monovalent metal binding sites that are conserved in class I and II human HDACs.[41,42] Site 1 and 2 are located 7 Å and 21 Å, respectively, from the divalent metal ion binding site and could be occupied by either K^+ or Na^+. Previous studies have revealed that MVCs bound to site 1 inhibits HDAC8 activity, likely by altering the pK_a of His-142, whereas occupation of MVC site 2 increases activity, likely by stabilizing the structure.[45] These MVC binding sites may also play a role in regulating metal selectivity and equilibrium kinetics. The metal dissociation kinetics of HDAC8 are influenced by the concentration of monovalent cations; K^+ and Na^+ decrease the Zn(II) dissociation rate constant by more than 40-fold and 12-fold, respectively, with no cooperativity. These data are consistent with a model in which MVCs bind to the high affinity site (site 1) to stabilize the active conformation of HDAC8 and thereby lower the metal dissociation rate constant.

Here we demonstrate that despite the differences in the binding affinity of HDAC8 for Zn(II) and Fe(II), the dissociation rate constants are comparable at 0.0006 s^{-1}. Furthermore, the metal binding kinetics suggest a two-step binding mechanism to HDAC8 where the metal selectivity is determined by the apparent slower association rate constant for Fe(II) compared with Zn(II). In the proposed model (Scheme 1) the association rate constant for Zn(II) is limited by formation of the encounter complex while the Fe(II) association rate constant includes both the encounter complex and the rearrangement step. Furthermore, these data indicate that the kinetics and thermodynamics of HDAC8 metal binding is dependent on the concentration and identity of both the divalent metal ions and the monovalent cations. These data are consistent with the proposal that HDAC8 could exist as an Fe(II)-dependent metalloenzyme as well as a Zn(II)-dependent enzyme depending on cellular factors.

Materials and Methods

Materials

Unless specified, chemicals and supplies were purchased from Fisher Scientific (MA). All chemicals were of the highest quality available. Ethylenediaminetetraacetic acid (EDTA), $FeCl_2$ (99.99%), and $Zn(NO_3)_2$ were purchased from Aldrich (MO). Chromatography resins were purchased from GE Healthcare. To prevent trace metal contamination, all plastic ware was presoaked with 1 m*M* EDTA and rinsed three times with Millipure H_2O. Plastic disposables, including pipet tips and microcentrifuge tubes, were certified trace metal-free (Corning Incorporated and Costar, respectively). Sodium hydroxide (Sigma, 99.999%) was used to titrate 3-(*N*-morpholino)propanesulfonic acid (MOPS) buffer (Ambion).

Expression and purification of HDAC8

Recombinant His_6-HDAC8 was expressed in BL21(DE3) *E. coli* transformed with pHD4 and

purified as previously described[13] and then concentrated to 2 to 5 mg/mL for metal exchange. Metal-free HDAC8 was generated by dialyzing purified HDAC8 twice into 500 mL of 25 m*M* MOPS (pH 7.0), 1 m*M* EDTA for 12 to 14 h at 4°C, followed by buffer exchange into 25 m*M* MOPS (pH 7.5), 0.1 m*M* EDTA, and then 25 m*M* MOPS (pH 7.5) once each for 12 to 14 h at 4°C. When necessary, anaerobic conditions were achieved using an anaerobic chamber (Coy, Grass Lake, MI). For Fe(II) experiments, a freshly made 10 m*M* $FeCl_2$ stock was prepared in 50 m*M* ascorbic acid and diluted to 100 μ*M* with 1× assay buffer (20 m*M* HEPES, pH 8, 3 m*M* KCl, 137 m*M* NaCl) before incubation with apo-HDAC8. Similarly, a 10 m*M* $ZnSO_4$ solution was prepared in 20 m*M* HEPES pH 8, 1 m*M* triscarboxyethylphosphine (TCEP) and diluted to 100 μ*M* with 1× assay buffer before incubation with apo-HDAC8.

Synthesis of fl-SAHA

Synthesis of 2-(3,6-dihydroxy-9H-xanthen-9-yl)−5-(8-methoxy-8-oxooctanamido)benzoic acid (1). To a flame-dried flask equipped with stir bar and dry DMF (10 mL) was added 6-fluoresceinamine (100 mg, 0.28 mmol, Sigma-Aldrich) in one portion (Fig. 2). Then dry triethylamine (Et_3N, 43 μL, 0.31 mmol) was added and the reaction was stirred at room temperature for 1 h. Methyl-8-chloro-1-oxooctanate (40 μL, 0.28 mmol) was then added to the solution drop wise and the reaction mixture was stirred at 50°C for 24 h. The solvent was then evaporated in vacuo and the residue was dissolved in dichloromethane (20 mL). The product was washed with sat. $NaHCO_3$ (3 × 20 mL) and NaCl (2 × 20 mL), dried over anhydrous $MgSO_4$, filtered and dried in vacuo to yield an orange-yellow oil. The product was purified via silica gel chromatography (4% MeOH in CH_2Cl_2) and the resulting product was washed with hexanes to remove residual impurities. The final product was an orange oil (yield: 81 mg, 0.16 mmol, 56%). ^{1}H NMR (CD_3OD, 400 MHz)/δ (ppm): 8.23 (d, J = 1.6 Hz, 1H), 7.73 (dd, J = 8.0, 2.0 Hz, 2H), 7.04 (d, J = 8.4 Hz, 2H), 6.56 (d, J = 2.4 Hz, 1H), 6.53 (d, J = 8.8 Hz, 2H), 6.43 (dd, J = 8.4, 2.4 Hz, 2H), 3.54 (s, 3H), 2.34 (t, J = 7.6, 2H), 2.24 (t, J = 7.6, 2H), 1.66–1.52 (m, 4H), 1.32–1.30 (m, 4H). $[M+H]^+$: calcd. = 518.13, Found = 518.06.

Synthesis of 2-(3,6-dihydroxy-9H-xanthen-9-yl)−5-(8-(hydroxyamino)−8-oxooctanamido)benzoic acid (fl-SAHA). Hydroxylamine hydrochloride (104 mg, 1.5 mmol) in methanol (10 mL) was combined with a solution of KOH (1.57 g, 28 mmol) in methanol (16 mL), cooled to 0°C, and then filtered. (**1**) was added to the filtrate and KOH (5 mg in 1 mL MeOH) was slowly added. The mixture was stirred at room temperature for 2 h and then refluxed at 65°C for 34 h. The reaction was quenched by the addition of cold water (15 mL), followed by drop-wise addition of glacial acetic acid until pH ~7.0. The precipitated solid product was filtered, washed with water to remove impurities, dried under vacuum, and purified twice by silica gel chromatography (25% MeOH in CH_2Cl_2). The final product was recrystallized in CH_2Cl_2 and hexanes to afford an orange solid (yield: 362 mg, 0.70 mmol, 75%). ^{1}H NMR (CD_3OD, 400 MHz)/δ (ppm): 8.24 (d, J = 1.6 Hz, 1H), 7.73 (dd, J = 8.0, 2.0 Hz, 2H), 7.04 (d, J = 8.4 Hz, 2H), 6.56 (d, J = 2.4 Hz, 1H), 6.53 (d, J = 8.8 Hz, 2H), 6.40 (dd, J = 8.4, 2.4 Hz, 2H), 2.32 (t, J = 7.6, 2H), 2.24 (t, J = 7.6, 2H), 1.68–1.51 (m, 4H), 1.37–1.33 (m, 4H). $[M+H]^+$: calcd. = 518.14, Found = 518.11.

Affinity of HDAC8 for fl-SAHA

FP experiments were performed in a half-area black 96-well microplate (Corning Incorporation, #3686) and FP values were measured with excitation at 485 nm (30 nm bandpass) and emission at 535 nm (40 nm bandpass) using a TECAN Plate Reader. Binding experiments for determining the K_D values of metal-bound HDAC8 for fl-SAHA included 50 n*M* fl-SAHA in assay buffer [20 m*M* HEPES (pH 8), 137 m*M* NaCl, 3 m*M* KCl] and FP was measured as HDAC8 (≤5 μ*M*) was titrated into the solution. The fluorescence intensity of fl-SAHA decreases by ~25% upon binding to HDAC8, even after correction for dilution and background fluorescence, as described previously.[67] The value of K_D for fl-SAHA was obtained by fitting a binding isotherm, including changes in the ligand concentration (L) due to binding to E, to the dependence of the FP signal on the concentration of HDAC8 [E, Eq. (1)]. In the equation, Pf is the polarization of unbound fl-SAHA and Pb is signal from the fl-SAHA·HDAC8 complex. All data analyses were performed using Prism 6.0 (GraphPad Software).

$$Y = Pf + (Pb\text{-}Pf) \times \frac{([L]+[E]+K_D) - \sqrt{([L]+[E]+K_D)^2 - 4[L][E]}}{2[E]} \quad (1)$$

Kinetics for binding fl-SAHA to HDAC8

Fluorescence stopped-flow measurements were carried out on a model SF-2001 stopped-flow spectrofluorometer (KinTek Corp., Austin, TX) fitted with a 75W xenon arc lamp in two syringe mode. fl-SAHA was excited at 495 nm (slit width, 0.1–2 mm) and fluorescence emission was monitored using a long-pass filter (N500nm; Corion, LL-500-F). All kinetic traces were an average of four to six independent determinations. To measure the dissociation rate constant (k_{off}), fl-SAHA (0.1 μ*M*) was preincubated with metal-bound HDAC8 (2 μ*M*) for at least 20 min

at RT in assay buffer. The reaction was initiated by mixing the HDAC8•fl-SAHA complex with an equal volume of unlabeled SAHA (final concentration of 20 μ*M*) in assay buffer at 25°C to trap HDAC8 and an increase in fluorescence intensity was measured. The dissociation rate constant was determined from a fit of a single exponential to the time-dependent changes in the fluorescence signal [Eq. (2)]. In the equation, ΔF is the observed change in fluorescence and ΔF_0 is the fluorescence at time zero.

$$\Delta F = \Delta F_0 \times \exp(-k_{off} \times t) \quad (2)$$

HDAC8 metal ion binding affinity

The affinity of HDAC8 for Zn(II) or Fe(II) was measured by assaying catalytic activity in the presence of varying $Me(II)_{free}$ concentrations in 1 m*M* nitrilotriacetic acid (NTA), 5 m*M* MOPS, pH 7, serving as both a pH and metal buffer in the presence of 3 m*M* KCl and 137 m*M* NaCl. The affinity was not dependent on NTA concentration (data not shown). Catalytic activity was assayed by using a commercially-available fluorescent assay (BIOMOL) with the Fluor de Lys (FdL) HDAC8 substrate (RHK(ac)K(ac)-methyl-coumarin). All assay buffers were pretreated with Chelex resin (Bio-Rad) to remove trace divalent metal ions. Metal-free HDAC8 variants were reconstituted with Zn(II) or Fe(II) by incubation with a stoichiometric concentration of metal in assay buffer (20 m*M* HEPES pH 8.0, 137 m*M* NaCl, 3 m*M* KCl, and 1 m*M* TCEP). The reaction was quenched by the addition of stoichiometric amounts of trichostatin A (TSA), a potent inhibitor of HDAC8. Fluorescence intensity was monitored at $\lambda_{ex} = 340$ and $\lambda_{em} = 450$ for the deacetylated and cleaved product, and at $\lambda_{ex} = 340$ and $\lambda_{em} = 380$ for the starting acetylated substrate. The ratio of product fluorescence divided by substrate fluorescence was observed and linearly increases with product concentration up to 30% product. The amount of product formed was determined from comparison to the fluorescence ratios of a standard curve made up of known concentrations of products and substrates. The linear initial rates catalyzed by wtHDAC8 in assay buffer at 25°C were measured.

The affinity of HDAC8 for the metal was also measured by changes in anisotropy by coupling the binding of fl-SAHA to metal binding. These reactions were carried out in 1× assay buffer containing 50 n*M* fl-SAHA. Fluorescence anisotropy assays were performed in a black 96-well microplate by monitoring the anisotropy signal of fluorescein ($\lambda_{ex} = 485$ nm and $\lambda_{em} = 535$ nm) using a TECAN plate-reader. For Zn(II) affinity measurements, apo-HDAC8 (1–200 μ*M*) was incubated with 1 m*M* NTA, 10 m*M* MOPS, pH 7, and 0 to 0.5 m*M* Zn_{tot} (0–3.3 n*M* Zn_{free}) at 25°C for 30 min.[12] The concentration of Zn_{free} in the metal buffers was calculated using the program MINEQL (Environmental Research software). For measurement of K_D for Fe(II), the assays contained 0 to 950 μ*M* total iron (Sigma, 99.99%, $Fe(II)_{free} = 0$–2.6 μ*M*, as calculated by MINEQL) and 1 μ*M* HDAC8, in the presence of 3 m*M* KCl and 137 m*M* NaCl. The assay mixtures were incubated for 2 h on ice to pre-equilibrate in the anaerobic glove box followed by addition of fl-SAHA and a short equilibration at 25°C before measuring the anisotropy signal. The Zn(II) and Fe(II) K_D values were obtained by fitting a binding isotherm to the dependence of either the activity or anisotropy on the concentration of Me_{free} [Eq. (3), *X*]. In the equation, *A* is the activity, Δ*A* is change in activity, FP is the fluorescence anisotropy, and ΔFP is the change in anisotropy.

$$\frac{A}{\Delta A} = \frac{FP}{\Delta FP} = \frac{X}{K_D \times X} \quad (3)$$

Metal ion dissociation rate constants

The first order rate constant for M(II) dissociation from HDAC8•M(II) complexes was measured by the time-dependent loss of activity upon incubation with EDTA. HDAC8 reconstituted with stoichiometric Zn(II) or Fe(II) (final concentration = 1 μ*M*) was diluted into assay buffer containing 1 m*M* EDTA at 25°C. At various times (0–60 min) an aliquot was diluted 10-fold into assay buffer containing 50 μ*M* FdL substrate. The reactions were quenched by the addition of TSA followed by trypsin developer. The initial rate for product formation was determined for each time point. The dissociation rate constant was determined from a single exponential fit to the decrease in the initial rate as a function of time.

Dependence of metal dissociation rate constant on monovalent cation (MVC) concentration

For measurement of the dependence of Zn(II) k_{off} on the concentration of MVC, reconstituted Zn(II)-HDAC8 was incubated with varying concentration of potassium or sodium ([KCl] = 1–100 m*M*, [NaCl] = 100–2000 m*M*) on ice for 1 h in 20 m*M* HEPES, pH 8.0 and then at 25°C for 4 min. The reaction was started by the addition of 1 m*M* EDTA. The dissociation rate constant of Zn(II) was measured from the decrease in catalytic activity using the FdL assay, as described above. The MVC dependence of k_{off} for Zn(II) was fit by Eq. (4), which is derived from the coupled binding of monovalent and divalent ions shown in Scheme 2. In the equation, K_{eq} is the apparent equilibrium constant for MVC binding and k_{off} is the dissociation rate constant for Zn(II).

$$k_{obs} = \frac{k_{off}}{1 + \frac{[MVC]^n}{K_{eq}^n}} \quad (4)$$

Acknowledgments

The authors gratefully acknowledge Dr. Ted Huston (University of Michigan Geological Sciences) for

assistance with ICP-MS analysis. The authors thank Dr. Anna Mapp and Dr. Aaron R. Van Dyke for generously providing materials for synthesis of fl-SAHA. Carol Fierke is the recipient of the Protein Society 2014 Emil Thomas Kaiser Award.

References

1. Strahl BD, Allis CD (2000) The language of covalent histone modifications. Nature 403:41–45.
2. Choudhary C, Kumar C, Gnad F, Nielsen ML, Rehman M, Walther TC, Olsen JV, Mann M (2009) Lysine acetylation targets protein complexes and co-regulates major cellular functions. Science 325:834–840.
3. Wolfson NA, Pitcairn CA, Fierke CA (2013) HDAC8 substrates: histones and beyond. Biopolymers 99:112–126.
4. Khochbin S, Verdel A, Lemercier C, Seigneurin-Berny D (2001) Functional significance of histone deacetylase diversity. Curr Opin Genet Dev 11:162–166.
5. Gregoretti IV, Lee YM, Goodson HV (2004) Molecular evolution of the histone deacetylase family: functional implications of phylogenetic analysis. J Mol Biol 338: 17–31.
6. Blander G, Guarente L (2004) The Sir2 family of protein deacetylases. Annu Rev Biochem 73:417–435.
7. Finnin MS, Donigian JR, Cohen A, Richon VM, Rifkind RA, Marks PA, Breslow R, Pavletich NP (1999) Structures of a histone deacetylase homologue bound to the TSA and SAHA inhibitors. Nature 401:188–193.
8. Marek M, Kannan S, Hauser AT, Moraes Mourão M, Caby S, Cura V, Stolfa DA, Schmidtkunz K, Lancelot J, Andrade L, Renaud JP, Oliveira G, Sippl W, Jung M, Cavarelli J, Pierce RJ, Romier C (2013) Structural basis for the inhibition of histone deacetylase 8 (HDAC8), a key epigenetic player in the blood fluke *Schistosoma mansoni*. PLoS Pathog 9:1–15.
9. Dowling DP, Gattis SG, Fierke CA, Christianson DW (2010) Structures of metal-substituted human histone deacetylase 8 provide mechanistic inferences on biological function. Biochemistry 49:5048–5056.
10. Dowling DP, Gantt SL, Gattis SG, Fierke CA, Christianson DW (2008) Structural studies of human histone deacetylase 8 and its site-specific variants complexed with substrate and inhibitors. Biochemistry 47: 13554–13563.
11. Vannini A, Volpari C, Gallinari P, Jones P, Mattu M, Carfi A, De Francesco R, Steinkuhler C, Di Marco S (2007) Substrate binding to histone deacetylases as shown by the crystal structure of the HDAC8-substrate complex. EMBO Rep 8:879–884.
12. McCall KA, Fierke CA (2004) Probing determinants of the metal ion selectivity in carbonic anhydrase using mutagenesis. Biochemistry 43:3979–3986.
13. Gantt SL, Gattis SG, Fierke CA (2006) Catalytic activity and inhibition of human histone deacetylase 8 is dependent on the identity of the active site metal ion. Biochemistry 45:6170–6178.
14. Christianson DW, Cox JD (1999) Catalysis by metal-activated hydroxide in zinc and manganese metalloenzymes. Annu Rev Biochem 68:33–57.
15. Auld DS (2001) Zinc coordination sphere in biochemical zinc sites. Biometals 14:271–313.
16. Hernick M, Fierke CA (2005) Zinc hydrolases: the mechanisms of zinc-dependent deacetylases. Arch Biochem Biophys 433:71–84.
17. Becker A, Schlichting I, Kabsch W, Groche D, Schultz S, Wagner AF (1998) Iron center, substrate recognition and mechanism of peptide deformylase. Nat Struct Biol 5:1053–1058.
18. Zhu J, Dizin E, Hu X, Wavreille AS, Park J, Pei D (2003) *S*-Ribosylhomocysteinase (LuxS) is a mononuclear iron protein. Biochemistry 42:4717–4726.
19. Gattis SG, Hernick M, Fierke CA (2010) Active site metal ion in UDP-3-O-((R)−3-Hydroxymyristoyl)-*N*-acetylglucosamine deacetylase (LpxC) switches between Fe(II) and Zn(II) depending on cellular conditions. J Biol Chem 285:33788–33796.
20. Hernick M, Gattis SG, Penner-Hahn JE, Fierke CA (2010) Activation of *Escherichia coli* UDP-3-O-[(R)−3-hydroxymyristoyl]-*N*-acetylglucosamine deacetylase by Fe2+ yields a more efficient enzyme with altered ligand affinity. Biochemistry 49:2246–2255.
21. Wegener D, Wirsching F, Riester D, Schwienhorst A (2003) A fluorogenic histone deacetylase assay well suited for high-throughput activity screening. Chem Biol 10:61–68.
22. Mazitschek R, Patel V, Wirth DF, Clardy J (2008) Development of a fluorescence polarization based assay for histone deacetylase ligand discovery. Bioorg Med Chem Lett 18:2809–2812.
23. Singh RK, Mandal T, Balasubramanian N, Cook G, Srivastava DK (2011) Coumarin-suberoylanilide hydroxamic acid as a fluorescent probe for determining binding affinities and off-rates of histone deacetylase inhibitors. Anal Biochem 408:309–315.
24. Kristoffersen AS, Erga SR, Hamre B, Frette O (2014) Testing fluorescence lifetime standards using two-photon excitation and time-domain instrumentation: rhodamine B, coumarin 6 and lucifer yellow. J Fluoresc 24:1015–1024.
25. Takagai Y, Nojiri Y, Takase T, Hinze WL, Butsugan M, Igarashi S (2010) "Turn-on" fluorescent polymeric microparticle sensors for the determination of ammonia and amines in the vapor state. Analyst 135:1417–1425.
26. Zheng H, Zhan XQ, Bian QN, Zhang XJ (2013) Advances in modifying fluorescein and rhodamine fluorophores as fluorescent chemosensors. Chem Comm 49: 429–447.
27. Martin MM, Lindqvist L (1975) pH-dependence of fluorescein fluorescence. J Lumin 10:381–390.
28. Irving H, Williams RJP (1948) Order of stability of metal complexes. Nature 162:746–747.
29. Outten CE, O'Halloran TV (2001) Femtomolar sensitivity of metalloregulatory proteins controlling zinc homeostasis. Science 292:2488–2492.
30. Wang D, Hosteen O, Fierke CA (2012) ZntR-mediated transcription of zntA responds to nanomolar intracellular free zinc. J Inorg Biochem 111:173–181.
31. Vinkenborg JL, Nicolson TJ, Bellomo EA, Koay MS, Rutter GA, Merkx M (2009) Genetically encoded FRET sensors to monitor intracellular Zn2+ homeostasis. Nat Methods 6:737–740.
32. Bozym RA, Thompson RB, Stoddard AK, Fierke CA (2006) Measuring picomolar intracellular exchangeable zinc in PC-12 cells using a ratiometric fluorescence biosensor. ACS Chem Biol 1:103–111.
33. Qin Y, Dittmer PJ, Park JG, Jansen KB, Palmer AE (2011) Measuring steady-state and dynamic endoplasmic reticulum and Golgi Zn2+ with genetically encoded sensors. Proc Natl Acad Sci USA 108:7351–7356.
34. Petrat F, de Groot H, Rauen U (2001) Subcellular distribution of chelatable iron: a laser scanning microscopic study in isolated hepatocytes and liver endothelial cells. Biochem J 356:61–69.
35. Meguro R, Asano Y, Odagiri S, Li C, Iwatsuki H, Shoumura K (2007) Nonheme-iron histochemistry for

light and electron microscopy: a historical, theoretical and technical review. Arch Histol Cytol 70:1–19.
36. Esposito BP, Epsztejn S, Breuer W, Cabantchik ZI (2002) A review of fluorescence methods for assessing labile iron in cells and biological fluids. Anal Biochem 304:1–18.
37. MacKenzie EL, Iwasaki K, Tsuji Y (2008) Intracellular iron transport and storage: from molecular mechanisms to health implications. Antioxid Redox Signal 10:997–1030.
38. Singh RK, Lall N, Leedahl TS, McGillivray A, Mandal T, Haldar M, Mallik S, Cook G, Srivastava DK (2013) Kinetic and thermodynamic rationale for suberoylanilide hydroxamic acid being a preferential human histone deacetylase 8 inhibitor as compared to the structurally similar ligand, trichostatin a. Biochemistry 52:8139–8149.
39. Pearson RG (1963) Hard and soft acids and bases. J Am Chem Soc 85:3533–3539.
40. Fersht AR (2000) Transition-state structure as a unifying basis in protein-folding mechanisms: contact order, chain topology, stability, and the extended nucleus mechanism. Proc Natl Acad Sci USA 97:1525–1529.
41. Vannini A, Volpari C, Filocamo G, Casavola EC, Brunetti M, Renzoni D, Chakravarty P, Paolini C, De Francesco R, Gallinari P, Steinkühler C, Di Marco S (2004) Crystal structure of a eukaryotic zinc-dependent histone deacetylase, human HDAC8, complexed with a hydroxamic acid inhibitor. Proc Natl Acad Sci USA 101:15064–15069.
42. Somoza JR, Skene RJ, Katz BA, Mol C, Ho JD, Jennings AJ, Luong C, Arvai A, Buggy JJ, Chi E, Tang J, Sang BC, Verner E, Wynands R, Leahy EM, Dougan DR, Snell G, Navre M, Knuth MW, Swanson RV, McRee DE, Tari LW (2004) Structural snapshots of human HDAC8 provide insights into the class I histone deacetylases. Structure 12:1325–1334.
43. Borin ML, Goldman WF, Blaustein MP (1993) Intracellular free Na+ in resting and activated A7r5 vascular smooth-muscle cells. Am J Physiol 264:C1513–C1524.
44. Woehl EU, Dunn MF (1995) The roles of Na+ and K+ in pyridoxal-phosphate enzyme catalysis. Coord Chem Rev 144:147–197.
45. Gantt SL, Joseph CG, Fierke CA (2010) Activation and inhibition of histone deacetylase 8 by monovalent cations. J Biol Chem 285:6036–6043.
46. Kasner SE, Ganz MB (1992) Regulation of intracellular potassium in mesangial cells: a fluorescence analysis using the dye, PBFI. Am J Physiol 262:F462–F467.
47. Borin ML, Goldman WF, Blaustein MP (1993) Intracellular free Na+ in resting and activated A7r5 vascular smooth muscle cells. Am J Physiol 264:C1513–C1524.
48. Tripp BC, Bell CB, 3rd, Cruz F, Krebs C, Ferry JG (2004) A role for iron in an ancient carbonic anhydrase. J Biol Chem 279:6683–6687.
49. D'Souza V M, Holz RC (1999) The methionyl aminopeptidase from *Escherichia coli* can function as an iron(II) enzyme. Biochemistry 38:11079–11085.
50. Porter DJ, Austin EA (1993) Cytosine deaminase. The roles of divalent metal ions in catalysis. J Biol Chem 268:24005–24011.
51. Seffernick JL, McTavish H, Osborne JP, de Souza ML, Sadowsky MJ, Wackett LP (2002) Atrazine chlorohydrolase from Pseudomonas sp. strain ADP is a metalloenzyme. Biochemistry 41:14430–14437.
52. Gattis SG (2010) Mechanism and metal specificity of zinc-dependent deacetylases. PhD. Thesis. University of Michigan, pp 143–145.
53. Waldron KJ, Rutherford JC, Ford D, Robinson NJ (2009) Metalloproteins and metal sensing. Nature 460: 823–830.
54. Rae TD, Schmidt PJ, Pufahl RA, Culotta VC, O'Halloran TV (1999) Undetectable intracellular free copper: the requirement of a copper chaperone for superoxide dismutase. Science 284:805–808.
55. O'Halloran TV, Culotta VC (2000) Metallochaperones, an intracellular shuttle service for metal ions. J Biol Chem 275:25057–25060.
56. Shi H, Bencze KZ, Stemmler TL, Philpott CC (2008) A cytosolic iron chaperone that delivers iron to ferritin. Science 320:1207–1210.
57. Nandal A, Ruiz JC, Subramanian P, Ghimire-Rijal S, Sinnamon RA, Stemmler TL, Bruick RK, Philpott CC (2011) Activation of the HIF prolyl hydroxylase by the iron chaperones PCBP1 and PCBP2. Cell Metab 14: 647–657.
58. Frey AG, Nandal A, Park JH, Smith PM, Yabe T, Ryu MS, Ghosh MC, Lee J, Rouault TA, Park MH, Philpott CC (2014) Iron chaperones PCBP1 and PCBP2 mediate the metallation of the dinuclear iron enzyme deoxyhypusine hydroxylase. Proc Natl Acad Sci USA 111:8031–8036.
59. Joshi P, Greco TM, Guise AJ, Luo Y, Yu F, Nesvizhskii AI, Cristea IM (2013) The functional interactome landscape of the human histone deacetylase family. Mol Syst Biol 9:1–21.
60. Thompson RB, Maliwal BP, Fierke CA (1998) Determination of metal ions by fluorescence anisotropy exhibits a broad dynamic range. Adv Opt Biophys 3256:51–59.
61. Suhling K, Siegel J, Lanigan PM, Leveque-Fort S, Webb SE, Phillips D, Davis DM, French PM (2004) Time-resolved fluorescence anisotropy imaging applied to live cells. Opt Lett 29:584–586.
62. Levitt JA, Matthews DR, Ameer-Beg SM, Suhling K (2009) Fluorescence lifetime and polarization-resolved imaging in cell biology. Curr Opin Biotechnol 20:28–36.
63. Wang D, Hurst TK, Thompson RB, Fierke CA (2011) Genetically encoded ratiometric biosensors to measure intracellular exchangeable zinc in *Escherichia coli*. J Biomed Opt 16:1–11.
64. Huang CC, Lesburg CA, Kiefer LL, Fierke CA, Christianson DW (1996) Reversal of the hydrogen bond to zinc ligand histidine-119 dramatically diminishes catalysis and enhances metal equilibration kinetics in carbonic anhydrase II. Biochemistry 35:3439–3446.
65. Kiefer LL, Paterno SA, Fierke CA (1995) Hydrogen-bond network in the metal-binding site of carbonic-anhydrase enhances zinc affinity and catalytic efficiency. J Am Chem Soc 117:6831–6837.
66. Hurst TK, Wang D, Thompson RB, Fierke CA (2010) Carbonic anhydrase II-based metal ion sensing: Advances and new perspectives. Biochim Biophys Acta 1804: 393–403.
67. Lohman TM, Mascotti DP (1992) Thermodynamics of ligand-nucleic acid interactions. Methods Enzymol 212: 400–424.